minor contribution to polymerization from the monomeric state. In contrast, the arms are of minor overall importance to binding but contribute to polymerization of monomeric actin when covalently attached to the globular domain.

These deletion results appear to segregate SipA function directly along structural lines. The ability of SipA to polymerize monomeric actin is dependent on the extended arms, which bind spatially distant actin molecules, whereas the globular core functions primarily to bind to preexisting filaments, probably because the core is unable to effectively tether molecules in opposing strands. In combination, the core and tethering arms enable SipA to both induce and stabilize the filamentous form of actin. This division of function provides an explanation for the ability of certain "one-armed" constructs to retain some ability to polymerize G-actin, because the core binding with an additional arm tethering may confer enough additional stability to the filament to enhance polymerization.

The presence of the "arm" nonglobular density may be expected to create a molecule with an elongated appearance in solution, as is observed by EM (*10*) in actin complexes with SipA$^{446-684}$ and by small-angle x-ray scattering (*13*). We determined the hydrodynamic radius of various SipA constructs (Fig. 3F) and found not only that the ordered core (as found in the crystals) was globular in solution but also that SipA constructs with additional polypeptide arms were elongated in solution and became increasingly elongated as more arm polypeptide was added (Fig. 3F). As estimated by the frictional coefficient, the larger SipA molecules were as elongated as fibronectin and tenascin (*14*).

To further probe this hypothesis of flexible polypeptides at the N- and C-termini of the molecule, we subjected a larger construct, SipA$^{425-684}$, to limited proteolysis with the relatively nonspecific protease subtilisin (Fig. 3E) (*11*). The protease cut very effectively until it approached a construct that was ordered in the crystals (SipA$^{513-657}$), producing trimmed constructs that when subcloned and overexpressed were highly soluble, stable, and active to bind F-actin (Fig. 3, E and F). These observations are consistent with a model that proposes a well-folded, protease-resistant globular domain with protease-sensitive polypeptides extending from its termini.

Thus, on the basis of our EM, proteolytic digestion, and hydrodynamic radius data, we show that the arm polypeptides that are critical to activity contribute to an elongated appearance in actin-SipA complexes, are associated with proteolytically accessible peptide, and elongate SipA in solution. Because eukaryotic proteins like nebulin are also elongated in tethering actin subunits in the filament, the lack of sequence or structural similarity between SipA and such host molecules indicates that it probably represents another case of convergent evolution in bacterial pathogenesis (*10*, *15*).

References and Notes

1. T. Pang, Z. A. Bhutta, B. B. Finlay, M. Altwegg, *Trends Microbiol.* **3**, 253 (1995).
2. T. J. Torok *et al.*, *JAMA* **278**, 389 (1997).
3. J. E. Galan, A. Collmer, *Science* **284**, 1322 (1999).
4. G. R. Cornelis, F. Van Gijsegem, *Annu. Rev. Microbiol.* **54**, 735 (2000).
5. J. E. Galan, D. Zhou, *Proc. Natl. Acad. Sci. U.S.A.* **97**, 8754 (2000).
6. R. M. Tsolis *et al.*, *Infect. Immun.* **68**, 3158 (2000).
7. S. Zhang *et al.*, *Infect. Immun.* **70**, 3843 (2002).
8. D. Zhou, M. S. Mooseker, J. E. Galan, *Science* **283**, 2092 (1999).
9. E. J. McGhie, R. D. Hayward, V. Koronakis, *EMBO J.* **20**, 2131 (2001).
10. V. E. Galkin *et al.*, *Nature Struct. Biol.* **9**, 518 (2002).
11. Materials and methods are available as supporting material on *Science* Online.
12. L. Holm, C. Sander, *J. Mol. Biol.* **233**, 123 (1993).
13. K. Mitra, D. Zhou, J. E. Galan, *FEBS Lett.* **482**, 81 (2000).
14. G. Schurmann, J. Haspel, M. Grumet, H. P. Erickson, *Mol. Biol. Cell* **12**, 1765 (2001).
15. N. Lukoyanova *et al.*, *Curr. Biol.* **12**, 383 (2002).
16. Figures were prepared with Molscript (*17*), Raster3D (*18*), Swiss-PdbViewer (*19*), and Ribbons (*20*).
17. P. J. Kraulis, *Appl. Crystallogr.* **24**, 946 (1991).
18. E. A. Merritt, D. J. Bacon, *Methods Enzymol.* **277**, 505 (1997).
19. N. Guex, M. C. Peitsch, *Electrophoresis* **18**, 2714 (December 1997).
20. M. M. Carson, *Methods Enzymol.* **277**, 493 (1997).

21. This work was funded by Public Health Services grants (to C.E.S. and E.H.E.) and through a Burroughs-Wellcome Investigators in Pathogenesis of Infectious Disease award to C.E.S. Coordinates have been deposited to the Protein Data Bank under ID code1Q5Z.

Supporting Online Material

www.sciencemag.org/cgi/content/full/301/5641/1918/DC1
Materials and Methods
Fig. S1
Table S1
References

25 June 2003; accepted 14 August 2003

R2D2, a Bridge Between the Initiation and Effector Steps of the *Drosophila* RNAi Pathway

Qinghua Liu,[1] Tim A. Rand,[1] Savitha Kalidas,[2] Fenghe Du,[1] Hyun-Eui Kim,[1] Dean P. Smith,[2] Xiaodong Wang[1]*

The RNA interference (RNAi) pathway is initiated by processing long double-stranded RNA into small interfering RNA (siRNA). The siRNA-generating enzyme was purified from *Drosophila* S2 cells and consists of two stoichiometric subunits: Dicer-2 (DCR-2) and a previously unknown protein that we named R2D2. R2D2 is homologous to the *Caenorhabditis elegans* RNAi protein RDE-4. Association with R2D2 does not affect the enzymatic activity of DCR-2. Rather, the DCR-2/R2D2 complex, but not DCR-2 alone, binds to siRNA and enhances sequence-specific messenger RNA degradation mediated by the RNA-initiated silencing complex (RISC). These results indicate that R2D2 bridges the initiation and effector steps of the *Drosophila* RNAi pathway by facilitating siRNA passage from Dicer to RISC.

RNA interference (RNAi) is a form of posttranscriptional gene silencing whereby double-stranded RNA (dsRNA) molecules trigger the sequence-specific degradation of cognate mRNA (*1–3*). The biological importance of RNAi is underscored by its wide conservation throughout metazoans and the existence of closely related systems in plants (called cosuppression) and fungi (called quelling) (*4*). Emerging evidence indicates that the RNAi and related pathways function in many fundamental biological processes, including antiviral defense, development, and maintenance of genomic stability (*4*).

The *Drosophila* RNAi pathway consists of initiation and effector steps. First, long dsRNA molecules are cleaved into 21- to 23-nucleotide (nt) small interfering RNA (siRNA) duplexes (*5–8*). Secondly, the siRNA is incorporated into a nuclease complex named RNA-initiated silencing complex (RISC) and functions as a guide RNA to direct RISC-mediated sequence-specific mRNA degradation (*6*, *9–11*). The endonucleases that process dsRNA have been identified as Dicers, a family of large noncanonical ribonuclease (RNase) III enzymes (*5*). Although only one Dicer enzyme is found in *Caenorhabditis elegans* and humans, two, DCR-1 and DCR-2, have

[1]Howard Hughes Medical Institute and Department of Biochemistry, [2]Department of Pharmacology and Center for Basic Neuroscience, University of Texas (UT) Southwestern Medical Center at Dallas, Dallas, TX 75390, USA.

*To whom correspondence should be addressed. E-mail: xwang@biochem.swmed.edu

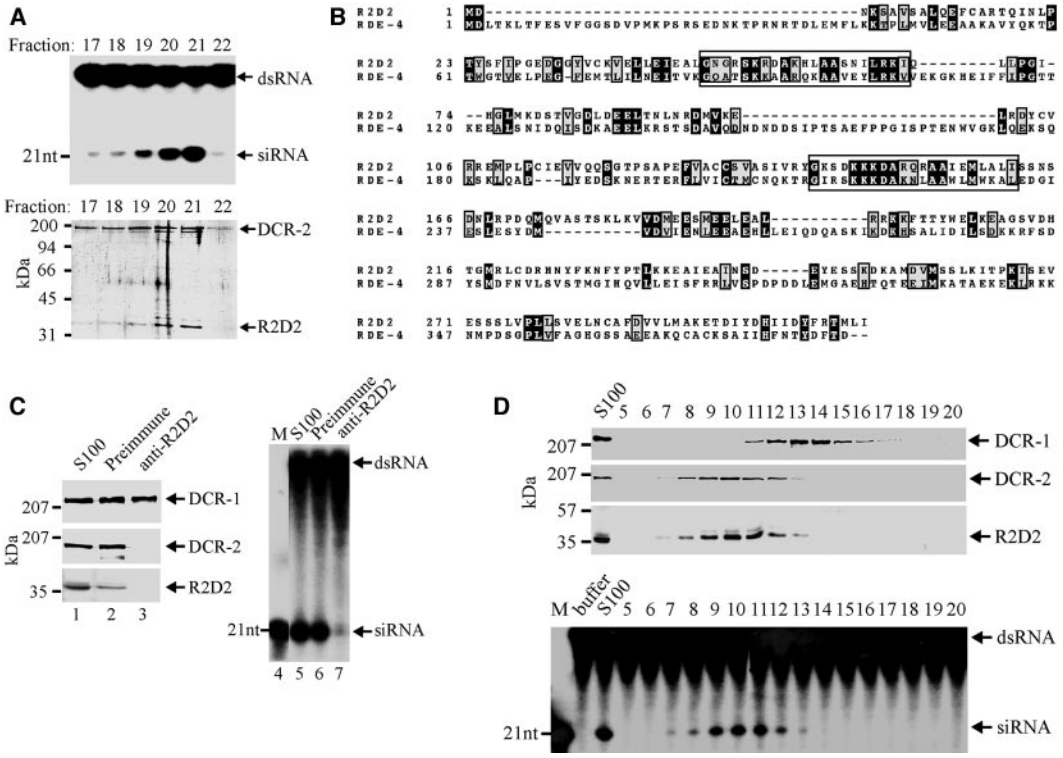

Fig. 1. (**A**) Purification of the siRNA-generating activity. Individual fractions from the final gel filtration column were assayed for Dicer activity (*12*) (top) or resolved by SDS–polyacrylamide gel electrophoresis (PAGE) followed by silver staining (bottom). Arrows indicate the positions of dsRNA and siRNA (top) or DCR-2 and R2D2 proteins (bottom). (**B**) A protein sequence alignment of R2D2 (*D. melanogaster*) and RDE-4 (*C. elegans*). The two consensus dsRNA-binding motifs are boxed. Identical residues are shaded in black and conserved residues in gray. (**C**) Immunodepletions were performed in S100 (lane 1 and 5) with the use of the preimmune serum (lane 2 and 6) or anti-R2D2 serum (lane 3 and 7). DCR-1, DCR-2, or R2D2 proteins were detected in the supernatants by Western blotting with the use of the corresponding antibody (left). The Dicer assays were carried out with 1 μl of each supernatant (right). A 21-nt radiolabeled siRNA marker (M) is shown in lane 4. (**D**) S100 was fractionated by a Q-Sepharose column. DCR-1, DCR-2, and R2D2 proteins were detected by Western blotting (top), whereas the siRNA-generating activities were measured among different fractions (bottom).

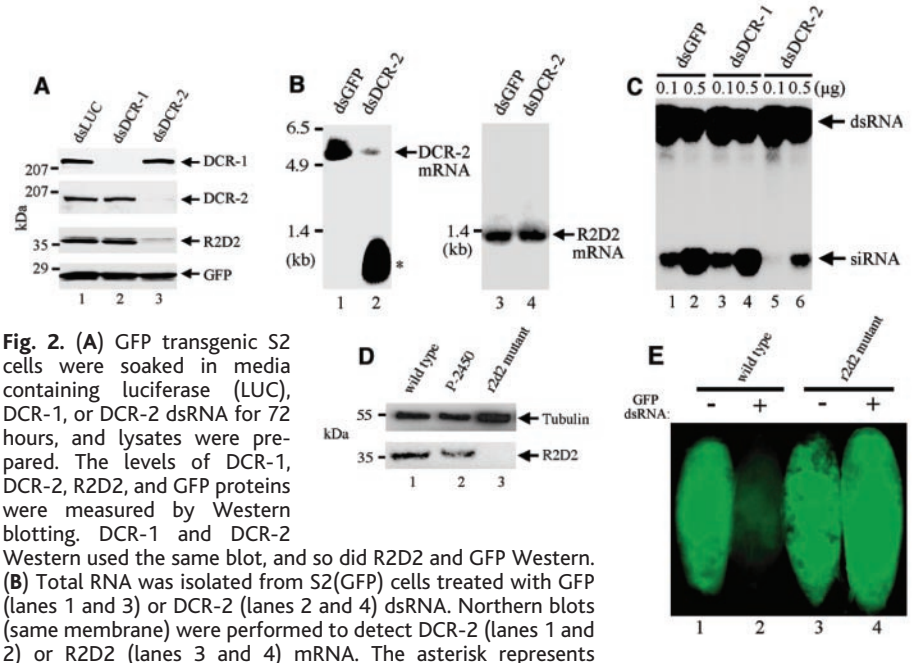

Fig. 2. (**A**) GFP transgenic S2 cells were soaked in media containing luciferase (LUC), DCR-1, or DCR-2 dsRNA for 72 hours, and lysates were prepared. The levels of DCR-1, DCR-2, R2D2, and GFP proteins were measured by Western blotting. DCR-1 and DCR-2 Western used the same blot, and so did R2D2 and GFP Western. (**B**) Total RNA was isolated from S2(GFP) cells treated with GFP (lanes 1 and 3) or DCR-2 (lanes 2 and 4) dsRNA. Northern blots (same membrane) were performed to detect DCR-2 (lanes 1 and 2) or R2D2 (lanes 3 and 4) mRNA. The asterisk represents degradation products of DCR2 mRNA. (**C**) The siRNA-generating activities were compared among lysates prepared from GFP (lanes 1 and 2), DCR-1 (lanes 3 and 4), or DCR-2 (lanes 5 and 6) dsRNA-treated S2 cells. (**D**) Lysates were prepared from wild-type flies (lane 1), the starting P element strain (lane 2), and the *r2d2* mutant flies derived by P element mobilization (lane 3). Western blots were performed with the use of antibody against R2D2 and antibody against α-tubulin as loading control. (**E**) Wild-type or *r2d2* mutant embryos expressing GFP were injected with GFP dsRNA. Images shown include a wild-type embryo injected with buffer (lane 1, –) or GFP dsRNA (lane 2, +) or an *r2d2* mutant embryo injected with buffer (lane 3, –) or GFP dsRNA (lane 4, +). In total, 46 of 52 wild-type embryos and 0 of 30 *r2d2* mutant embryos showed silencing of GFP expression.

been identified in *Drosophila* (*5*). It remains unclear how siRNA is transferred from Dicer to RISC.

We studied this problem by purifying the siRNA-generating activity from the cytoplasmic (S100) extract of S2 cells through a six-step chromatographic procedure (*12*). A single major peak of activity was observed at all steps and was followed throughout purification. Two proteins, ~190 kD and ~36 kD, showed perfect correlation with the enzymatic activity after the final gel filtration step (Fig. 1A). They were identified by mass spectrometry to be DCR-2 and a previously unknown protein (Flybase CG7138), respectively. We named this protein R2D2 because it contains two dsRNA-binding domains (R2) and is associated with DCR-2 (D2). R2D2 bears 20.9% identity and 33.4% similarity to the *C. elegans* RNAi protein RDE-4, which also contains tandem dsRNA-binding domains and interacts with Dicer (Fig. 1B) (*13*, *14*).

To confirm our purification results, we performed immunodepletion experiments with antiserum directed against the carboxyl-terminal 150 amino acids of R2D2. This R2D2 antibody depleted both R2D2 and DCR-2 proteins and removed the majority of siRNA-generating activity from S100, whereas the level of DCR-1 remained unchanged in the supernatant (Fig. 1C). Furthermore, when S100 was fractionated on a Q-Sepharose column (Amersham), DCR-2 and

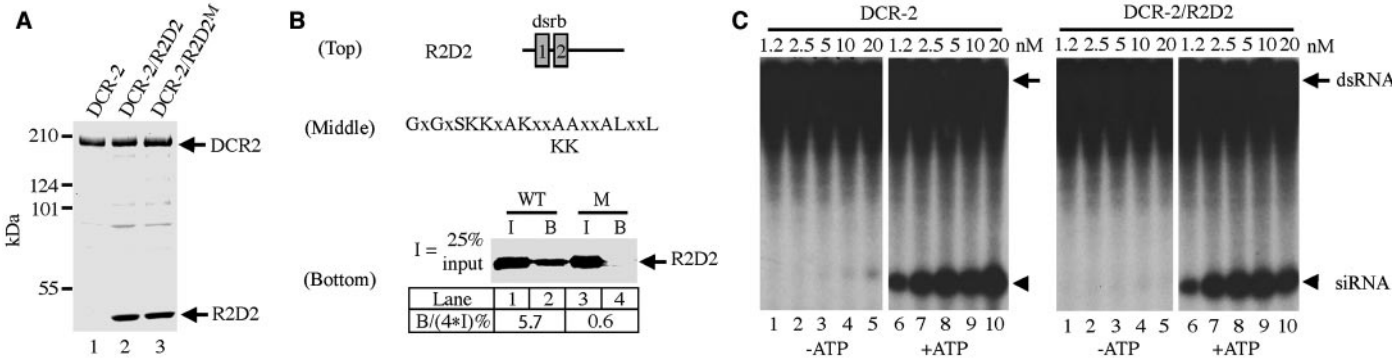

Fig. 3. (**A**) A Coomassie-stained SDS-PAGE gel showing purified recombinant DCR-2 (lane 1), wild-type DCR-2/R2D2 (lane 2), or mutant DCR-2/R2D2^{M} complex proteins. (**B**) (Top) A schematic diagram of the domain structure of R2D2 protein. The shaded boxes refer to dsRNA-binding (dsrb) domains. (Middle) The consensus dsrb motif sequence is shown. Two conserved alanines (A) were substituted by lysines (K) in both dsrb motifs in the mutant R2D2 protein. G, glycine; S, serine; L, leucine; and x, any amino acid. (Bottom) A dsRNA-binding assay by using poly (inosine):poly (cytidine)-conjugated beads to precipitate in vitro–translated ^{35}S-labeled wild-type (WT, lanes 1 and 2) and mutant (M, lanes 3 and 4) R2D2 protein (12). Twenty-five percent of input (I) and all of bound (B) proteins were resolved by SDS-PAGE, detected and quantified by phosphorimaging. The percentage of bound/input protein is indicated below the lanes. (**C**) DCR-2 is ATP-dependent and shows equivalent siRNA-generating activity as DCR2/R2D2. The concentration of recombinant proteins was measured by Bradford assay and indicated above the lanes. Dicer assays were performed in the absence (lanes 1 to 5) or presence (lanes 6 to 10) of ATP. Arrows indicate dsRNA and arrowheads, siRNA. (**D**) DCR-2/R2D2^{M} is as active as the wild-type complex. A series of dilutions of wild-type DCR-2/R2D2 (lanes 1 to 5) and mutant DCR-2/R2D2^{M} (lanes 6 to 10) complex proteins were compared for Dicer activity in the presence of ATP.

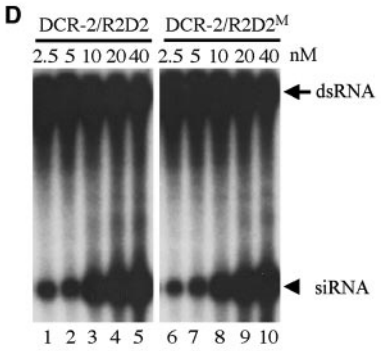

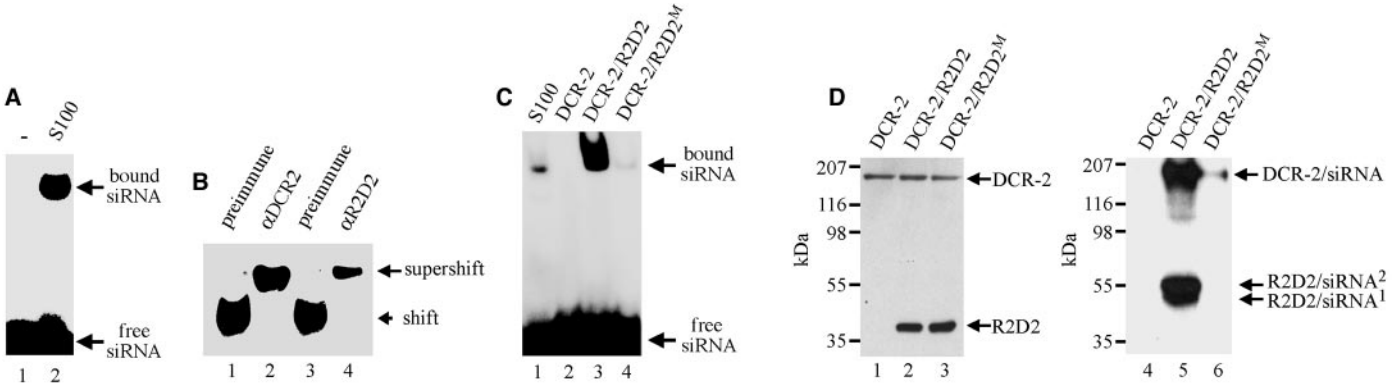

Fig. 4. (**A**) A gel shift assay showing a siRNA-binding activity in S100 (*12*). Radiolabeled siRNA was incubated with buffer alone (lane 1) or 40 μg of S100 (lane 2) in the absence of ATP. (**B**) Gel shift assays were performed in the presence of antibodies against DCR-2 (lane 2) or R2D2 (lane 4), or their preimmune sera (lanes 1 and 3). Short and long arrows indicate the mobility shift and supershift, respectively. The free siRNA ran off the gel. (**C**) Gel shift assays were performed with 5 μg of S100 (lane 1) and ~250 ng of purified DCR-2 (lane 2), DCR-2/R2D2 (lane 3), or DCR-2/R2D2^{M} (lane 4) recombinant proteins in the absence of ATP. (**D**) Gel shift assays were performed as in (C) but with the presence of ATP to decrease nonspecific crosslinking after UV exposure (*12*), resolved by SDS-PAGE, transferred to a cellulose membrane, and exposed to x-ray film (lanes 4 to 6). The same membrane was Western blotted with the antibody against His (lanes 1 to 3). Arrows indicate the positions of DCR-2 and R2D2 (lanes 1 to 3), or siRNA-crosslinked DCR-2 and R2D2 (lanes 4 to 6). The siRNA^{1} and siRNA^{2} refer to one or two strands of siRNA, respectively. (**E**) Wild-type DCR-2/R2D2 complex was used for the gel shift assay and UV crosslinking. Half of the reaction was treated with RNase A/T1, and half was untreated. Arrows and arrowheads refer to DCR-2 and R2D2 proteins that are crosslinked to full-length or RNase-digested siRNA, respectively.

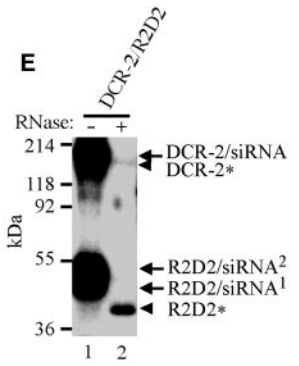

R2D2, but not DCR-1, correlated perfectly with the siRNA-generating activity (Fig. 1D).

To determine the contribution of DCR-1 and DCR-2 to siRNA production in *Drosophila* cells, we depleted either protein from S2 cells by dsRNA soaking (Fig. 2A). Interestingly, DCR-2 dsRNA also caused a substantial reduction in the level of R2D2 protein. This was not simply due to cross-targeting because the level of R2D2 mRNA was unaffected (Fig. 2B). Likewise, R2D2 dsRNA also reduced, although not as dramatically, the level of DCR-2 protein (*15*). These results indicate that DCR-2 and R2D2 form a stable complex and that either protein alone is unstable. Although depletion of DCR-1 made no difference, knocking down DCR-2 reduced the siRNA-generating activity by fivefold in lysates and interfered with RNAi in vivo (Fig. 2C and fig. S1). Together, these results demonstrate that the DCR-2/R2D2 complex is the principal siRNA-generating enzyme responsible for initiation of RNAi in *Drosophila* S2 cells.

To determine whether R2D2 is required for RNAi in vivo, we generated *r2d2* deletion mutant flies by P element mobilization (Fig. 2D) and crossed them with transgenic flies expressing green fluorescent protein (GFP) under the ubiquitin promoter to derive homozygous *r2d2; Ub-GFP* mutant flies (*16*). We then collected 0- to 2-hour wild-type or *r2d2* mutant embryos for microinjection of GFP dsRNA. Whereas introduction of GFP dsRNA effectively silenced GFP expression in wild-type embryos, *r2d2* mutant embryos were completely defective for the dsRNA-initiated RNAi response (Fig. 2E).

The siRNA-generating activity was reconstituted in vitro with the use of purified His_6-tagged DCR-2 and R2D2 recombinant proteins expressed in insect cells (Fig. 3A). A mutant form of R2D2 was also created by point mutations in the dsRNA-binding domains that abolish its ability to bind dsRNA (Fig. 3B). As shown in Fig. 3C, DCR-2 protein alone efficiently cleaved dsRNA into siRNA in an adenosine triphosphate (ATP)– and dose-dependent manner. The DCR-2/R2D2 complex was also ATP-dependent and showed activity equivalent to DCR-2 alone. We also performed kinetic studies with DCR-2 and DCR-2/R2D2 recombinant proteins and found no statistically significant difference in their K_m (a measure of substrate affinity) or K_{cat} (a measure of catalytic activity) (*15*). Furthermore, the mutant DCR-2/R2D2^M complex was as active in siRNA production as the wild-type complex (Fig. 3D). These results indicate that association with R2D2 does not affect the ability of DCR-2 to recruit or cleave dsRNA. This finding is inconsistent with the proposed function of RDE-4 to recruit dsRNA to DCR-1 (the single Dicer in worms) for processing (*13*). However, R2D2 may stabilize DCR-2 and thereby positively regulate siRNA production in *Drosophila* cells. Consistently, DCR-2 and R2D2 were expressed at much higher levels in insect cells when expressed jointly than separately (*15*).

To follow the fate of siRNA, we developed a gel shift assay to identify proteins that interact with siRNA. When radiolabeled synthetic siRNA was incubated with S2 lysate, a distinct mobility shift was observed on a native polyacrylamide gel (Fig. 4A). The formation of this siRNA-protein complex did not require ATP hydrolysis because it could be carried out efficiently at 4°C (*15*). Furthermore, when S100 was fractionated by a Q-Sepharose column, the peak of siRNA-binding activity correlated well with that of the siRNA-generating activity (*15*). We then performed the gel shift assays in the presence of antibodies against DCR-2 or R2D2. Both antibodies resulted in a supershift that was absent when their preimmune sera were used instead (Fig. 4B). This indicated that DCR-2 and R2D2 were present in this siRNA-protein complex.

Purified DCR-2, DCR-2/R2D2, and DCR-2/R2D2^M recombinant proteins were examined for siRNA binding by the gel shift assay. As shown in Fig. 4C, wild-type DCR-2/R2D2 complex, but not DCR-2 alone, bound to siRNA and produced a mobility shift indistinguishable from that of S100. The ability of the DCR-2/R2D2 complex to bind siRNA was greatly diminished by point mutations within the two dsRNA-binding domains of R2D2 (Fig. 4C, lanes 3 and 4). Thus, R2D2 is important for binding to the product (siRNA) rather than the substrate (dsRNA) of DCR-2.

Furthermore, when DCR-2/R2D2 proteins and radiolabeled siRNA were exposed to ultraviolet (UV) light, both DCR-2 and R2D2 were crosslinked to siRNA (Fig. 4D, lanes 4

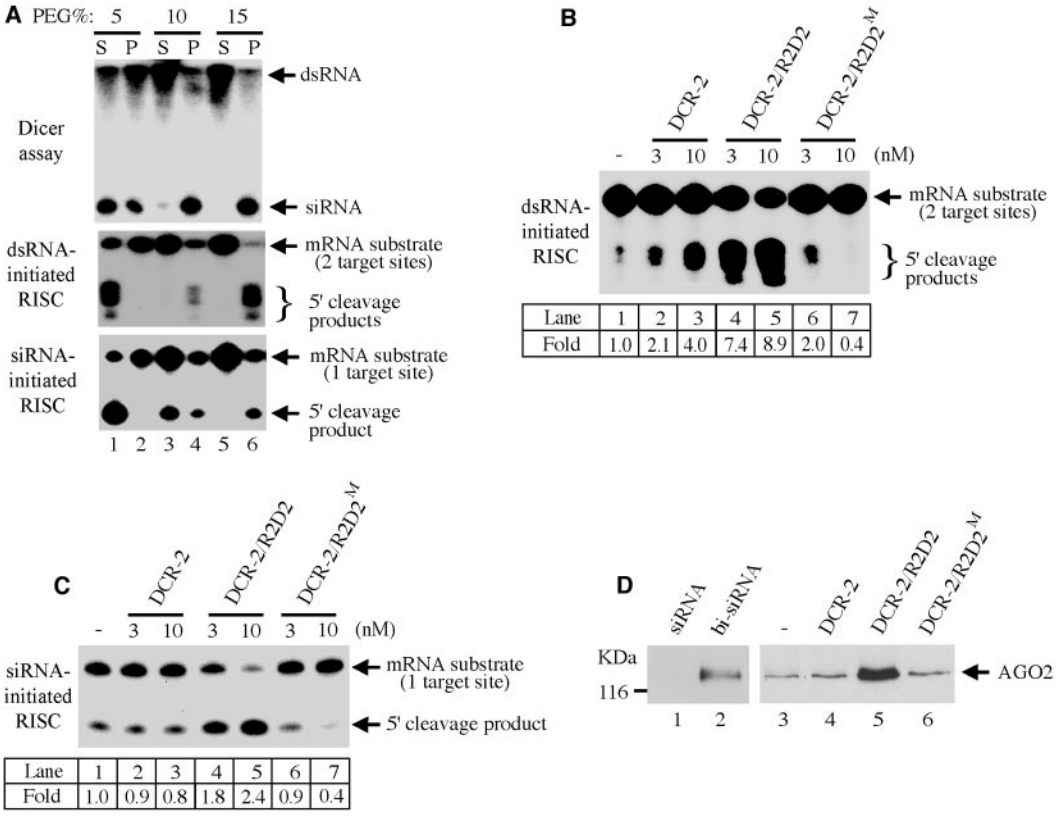

Fig. 5. (**A**) Partial purification of RISC. The Dicer assays (top) and the dsRNA- (middle) and siRNA-initiated (bottom) RISC assays were performed with the use of the supernatant (S) or pellet resuspension (P) of 5% (lanes 1 and 2), 10% (lanes 3 and 4), and 15% (lanes 5 and 6) PEG precipitation. The initiation time was 45 min at 30°C. For siRNA-initiated RISC assays, a ~200-nt mRNA substrate containing a single let-7 target site was radiolabeled at the 5′ cap and used as previously described (*17*). The 5′ cleavage product is ~115 nt. For dsRNA-initiated RISC assays, a radiolabeled mRNA containing tandem let-7 target sites was used to ensure maximal RISC activity. The 5′ cleavage products range from ~100 to 150 nt. The 130-bp dsRNA (3 nM) used to trigger RISC activity contained four direct repeats of the let-7 sequence. (**B**) The dsRNA-initiated RISC assays were performed in 10% PEG supernatant alone (lane 1) or in combination with 3 nM or 10 nM of recombinant DCR-2 (lanes 2 and 3), DCR-2/R2D2 (lanes 4 and 5), or DCR-2/R2D2^M (lanes 6 and 7) proteins. The incubation time is 90 min at 30°C. RISC activity equals the amount of product divided by the sum of the amounts of product + remaining substrate. The relative activity (Fold) was calculated by comparing the activity of each lane to that of lane 1. (**C**) The siRNA-initiated RISC assays were performed and analyzed as described in (B), except 25 nM siRNA was used and the incubation time was 45 min at 30°C. (**D**) RISC reactions were performed with 25 nM unmodified (lane 1) or biotinylated (lane 2) siRNA in S100, or with biotinylated siRNA in 10% PEG supernatant alone (lane 3) or in combination with 10 nM DCR-2 (lane 4), DCR-2/R2D2 (lane 5), or DCR-2/R2D2^M (lane 6) recombinant proteins. The biotinylated siRNA and associated proteins were precipitated by streptavidin beads, resolved by SDS-PAGE, and Western blotted for AGO2 (*12*).

to 6). This crosslinking was greatly diminished when the mutant DCR-2/R2D2^{M} complex was used instead, although similar amounts of proteins were used (Fig. 4D). Interestingly, we observed two R2D2-siRNA crosslinked bands, one at ~45 kD and another at ~52 kD, which probably represented R2D2 proteins covalently linked to one or two siRNA strands (the mass of each 21-nt siRNA strand was ~7 kD) (Fig. 4D, lane 5). This was confirmed by the downshift of both R2D2-siRNA crosslinked bands to the original position of ~38 kD His_6-R2D2 protein after RNase treatment (Fig. 4E). These results indicate that DCR-2 and R2D2 bind siRNA coordinately, which is dependent upon the dsRNA-binding domains of R2D2.

On the basis of this finding, we hypothesized that R2D2 might be involved in facilitating siRNA loading onto RISC. To test this hypothesis, we separated the RISC activity from the Dicer activity in S100 by polyethylene glycol (PEG) precipitation and then combined the partially purified RISC with recombinant Dicer proteins to reconstitute the RNAi reaction. As shown in Fig. 5A, although the majority of siRNA-generating activity was precipitated by 10% PEG, a substantial amount of RISC remained in the supernatant, which could be activated by addition of siRNA for sequence-specific mRNA degradation. The wild-type DCR-2/R2D2 complex was much more effective than DCR-2 alone or the mutant complex in promoting the dsRNA-initiated RISC activity in the 10% PEG supernatant (Fig. 5B). At 3 nM concentrations, wild-type DCR-2/R2D2 stimulated the RISC activity by more than sevenfold, whereas DCR-2 or DCR-2/R2D2^{M} stimulated only by twofold (Fig. 5B; compare lanes 2, 4, 6, and 1). Interestingly, the mutant complex blocked the RISC activity at 10 nM concentration, possibly as a result of dominant-negative effects (Fig. 5B; compare lanes 7 and 1). Furthermore, a similar phenomenon was observed in the siRNA-initiated RISC assay (Fig. 5C). Thus, the DCR-2/R2D2 complex could enhance the siRNA- as well as the dsRNA-initiated RISC activities. We further showed that this enhancement was not simply because of siRNA stabilization by DCR-2/R2D2 by comparing the stability of radiolabeled siRNA in the RISC reactions described above (*15*).

To confirm that DCR-2/R2D2 facilitates siRNA loading onto RISC, we followed the association between AGO2, an essential component of RISC, and a 3′-biotinylated siRNA by precipitation using streptavidin beads. The biotinylated siRNA was as active as unmodified siRNA in inducing RISC activities in S100 (*15*). However, streptavidin beads only precipitated AGO2 protein when biotinylated siRNA was used, suggesting that it was a specific interaction (Fig. 5D, lanes 1 and 2). We then performed RISC assays with the use of biotinylated siRNA in 10% PEG supernatant alone or in combination with recombinant DCR-2, DCR-2/R2D2, and DCR-2/R2D2^{M} proteins. Consistently, more AGO2 proteins were detected in the biotinylated siRNA precipitates when wild-type DCR-2/R2D2 complex was used instead of DCR-2 alone or the mutant complex. Together, our results indicate that DCR-2/R2D2 not only generates siRNA from dsRNA but also binds to nascent siRNA and facilitates its loading onto RISC. The latter activity is dependent on the dsRNA-binding domains of R2D2.

This model is supported by previous studies in which the direction of dsRNA processing was limited to one end of the dsRNA molecule (*11*). In these experiments, if dsRNA was processed from the 5′ to 3′ direction of the sense strand, it would generate RISC that can mediate degradation of the sense but not antisense target mRNA, and vice versa. However, if synthetic siRNA was used instead, it produced RISC that could degrade either sense or antisense target mRNA. Therefore, the newly synthesized symmetric siRNA product must not become a free molecule once it is generated from dsRNA. Rather, the nascent siRNA is likely to be retained by DCR-2/R2D2 in a fixed orientation determined by the direction of dsRNA processing such that only the antisense strand can become the guiding RNA for RISC.

Both R2D2 and RDE-4 contain tandem dsRNA-binding domains, interact with Dicer, and are required for the RNAi pathway (*13*, *14*). Thus, we conclude that R2D2 is homologous to RDE-4. RDE-4 also interacts with RDE-1, an AGO2 homolog and a RISC component. Therefore, we propose that R2D2 and RDE-4 play a similar role in bridging the initiation and effector steps of the *Drosophila* and *C. elegans* RNAi pathways, respectively.

References and Notes

1. A. Fire *et al*., *Nature* **391**, 806 (1998).
2. M. K. Montgomery, S. Xu, A. Fire, *Proc. Natl. Acad. Sci. U.S.A.* **95**, 15502 (1998).
3. T. Tuschl, P. D. Zamore, R. Lehmann, D. P. Bartel, P. A. Sharp, *Genes Dev.* **13**, 3191 (1999).
4. G. J. Hannon, *Nature* **418**, 244 (2002).
5. E. Bernstein, A. A. Caudy, S. M. Hammond, G. J. Hannon, *Nature* **409**, 363 (2001).
6. P. D. Zamore, T. Tuschl, P. A. Sharp, D. P. Bartel, *Cell* **101**, 25 (2000).
7. S. M. Elbashir, J. Martinez, A. Patkaniowska, W. Lendeckel, T. Tuschl, *EMBO J.* **20**, 6877 (2001).
8. A. Nykanen, B. Haley, P. D. Zamore, *Cell* **107**, 309 (2001).
9. S. M. Hammond, S. Boettcher, A. A. Caudy, R. Kobayashi, G. J. Hannon, *Science* **293**, 1146 (2001).
10. S. M. Hammond, E. Bernstein, D. Beach, G. J. Hannon, *Nature* **404**, 293 (2000).
11. S. M. Elbashir, W. Lendeckel, T. Tuschl, *Genes Dev.* **15**, 188 (2001).
12. Materials and methods are available as supporting material on *Science* Online.
13. H. Tabara, E. Yigit, H. Siomi, C. C. Mello, *Cell* **109**, 861 (2002).
14. A. Grishok, H. Tabara, C. C. Mello, *Science* **287**, 2494 (2000).
15. Q. Liu *et al*., unpublished data.
16. S. Kalidas *et al*., in preparation.
17. G. Hutvagner, P. D. Zamore, *Science* **297**, 2056 (2002); published online 1 August 2002; 10.1126/science.1073827.

18. We thank G. Hannon, E. Bernstein, J. Abrams, and L. Ford (Ambion) for useful reagents; H. Shu for mass spectrometric analysis; J. Morse for embryo injections; and J. Goldstein, K. Lynch, J. Rutter, X. Jiang, L. Wang, and P. Mishra for critical reading of the manuscript. This work was supported by a high-risk grant from UT Southwestern Medical Center and by grants from the American Heart Association (EI0040029N) and NIH (DC02539). T.A.R. is in the medical scientist training program. Q.L. is a GlaxoSmithKline Fellow of the Damon Runyon Cancer Research Foundation.

Supporting Online Material

www.sciencemag.org/cgi/content/full/301/5641/1921/DC1
Materials and Methods
Fig. S1
References and Notes

2 July 2003; accepted 13 August 2003

Epidermal Viral Immunity Induced by CD8α^{+} Dendritic Cells But Not by Langerhans Cells

Rhys S. Allan,[1]* Chris M. Smith,[2,3]* Gabrielle T. Belz,[2,3]* Allison L. van Lint,[1] Linda M. Wakim,[1] William R. Heath,[2,3]† Francis R. Carbone[1]†

The classical paradigm for dendritic cell function derives from the study of Langerhans cells, which predominate within skin epidermis. After an encounter with foreign agents, Langerhans cells are thought to migrate to draining lymph nodes, where they initiate T cell priming. Contrary to this, we show here that infection of murine epidermis by herpes simplex virus did not result in the priming of virus-specific cytotoxic T lymphocytes by Langerhans cells. Rather, the priming response required a distinct CD8α^{+} dendritic cell subset. Thus, the traditional view of Langerhans cells in epidermal immunity needs to be revisited to accommodate a requirement for other dendritic cells in this response.

Langerhans cells (LCs) represent the dominant dendritic cell (DC) subset within the skin epidermis (*1*). They are a mobile cell population capable of efficient antigen capture (*2*) and migration out of the skin on activation by a variety of stimuli (*3*–*5*). At the

R2D2, a Bridge Between the Initiation and Effector Steps of the *Drosophila* RNAi Pathway

Qinghua Liu, Tim A. Rand, Savitha Kalidas, Fenghe Du, Hyun-Eui Kim, Dean P. Smith and Xiaodong Wang

Science **301** (5641), 1921-1925.
DOI: 10.1126/science.1088710